High Step-Up High-Frequency Zero-Voltage Switched GaN-Based Single-Stage Isolated DC-DC Converter for PV Integration and Future DC Grids

Armin Jafari, Power and Wide-band-gap Electronics Research Laboratory (POWERlab), École polytechnique fédérale de Lausanne (EPFL), Switzerland, armin.jafari@epfl.ch
Elison Matioli, Power and Wide-band-gap Electronics Research Laboratory (POWERlab), École polytechnique fédérale de Lausanne (EPFL), Switzerland, elison.matioli@epfl.ch

Abstract

In this work we demonstrate a high step-up single-stage DC-DC micro-converter for photovoltaic (PV) applications. To reduce the size of passive components and the overall system, the circuit was designed to work at a high switching frequency of 300 kHz, by relying on GaN power HEMTs. To reach the high step-up ratio required in this type of applications, we designed a high-frequency planar transformer with high turns ratio, which enabled a high boost of voltage in just a single-stage DC-DC converter with a phase-shifted full-bridge (PSFB) topology, reaching an efficiency of more than 93%.

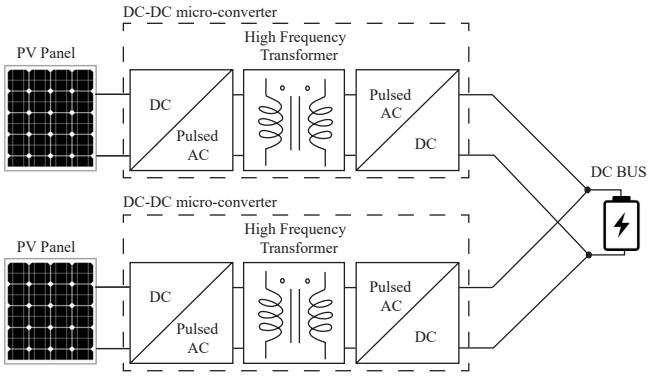

Fig. 1: The concept of micro-converter; a promising approach for tracking maximum power point locally in PV systems and overcoming the shading problem of panels

1. Introduction

A common approach used in PV systems to increase the DC link voltage required by a central inverter is to connect the PV panels in series. The disadvantage of this approach is that a single shaded panel degrades the power extracted from the whole string. Although there are methods to optimize the PV performance in partial shading conditions [1], there is still a huge loss of extracted power from a partially-shaded PV string. Paralleling PV panels with dedicated micro-converters is a promising approach to ensure that the maximum power is extracted from each panel, which in turn can recover up to 30% of the annual performance losses in PV systems [2]. This can be achieved with: 1. Micro-inverters, which utilize a dedicated inverter to connect each panel directly to the grid; 2. DC-DC micro-converters, which connect each panel to a DC bus, offering the flexibility to use a single central inverter for all the PV panels; in this case, a local maximum power point tracking (MPPT) can be realized with the economical benefit of using a single inverter. This concept, illustrated in Fig. 1, is also beneficial for future DC micro-grids relying on PVs as the primary source of power [3]-[4].

The main challenge of such micro-converters is to achieve a high voltage step-up with high efficiency. In this work, we present a high-efficiency high step-up single-stage DC-DC micro-converter using a PSFB topology. The high voltage step-up was achieved with a planar transformer with a high turns ratio of 1:12. A high switching frequency of 300 kHz was chosen to reduce the size of passive components and of the overall system, which is very important for the integration of micro-converters with PV panels. This was made possible by the use of GaN power HEMTs due to their small switching losses at high frequencies. We also discuss the unique advantages of the selected topology, such as zero-voltage switching (ZVS), zero-current switching (ZCS), and simplicity of implementation, combined with a compact design of the

This work was supported in part by the Swiss Office of Energy under Grant SI/501887-01 (MEPCO).

ISBN 978-3-8007-4646-0

high-frequency transformer, which led to superior thermal performance.

2. Topology

Among the categories of DC-DC converters, non-isolated topologies typically present lower efficiencies and limited control over the output voltage [5]. Isolated topologies, on the other hand, use transformers to provide galvanic isolation, which also allows a significant voltage step-up in a single-stage converter, suitable for the connection of a single PV panel to the higher voltage DC grid. Several high step-up converters have been introduced in literature, for example a LLC resonant converter [6], however, the efficiency of LLC converters is degraded if a high gain range is demanded [7]. By cascading a conventional boost converter with a LLC [5] one can reach a high step-up with a two-step voltage boost, which in turn adds to the complexity of design, modulation and control of the converter. In this work, we chose a phase-shifted full-bridge topology, shown in Fig. 2, which offers a high voltage step-up with a simple circuit and modulation [8]. The input DC voltage is first converted to high-frequency pulsed AC in the primary side inverter (left bridge). The high frequency transformer T1 provides the required voltage step up, and on the secondary side (right bridge), a full-wave rectifier generates the DC output voltage. There are several advantages of this topology, such as: 1. Simple modulation based on the phase shift between the gate signals of the two legs in the inverter, without changing the carrier frequency; 2. Inherent soft-switching (ZVS on turn-on and ZCS on turn-off) by using the leakage inductance of the transformer; in addition the low output capacitance of GaN switches improves the light load performance; 3. The high-frequency transformer provides galvanic isolation and enables high voltage step-up in a single stage. The parameters of the designed micro-converter are listed in Tab. 1. In the next section, we will discuss about the design of high-frequency transformer, as the key component for achieving high voltage step-up.

3. Design of high-frequency transformer

The design of the transformer plays a critical role in this topology, as it is responsible for the high step-up in the voltage level as well as providing the isolation between primary and secondary. In addition, its leakage inductance contributes for soft-switching of primary-side switches. We chose to design a planar transformer due to their compactness, excellent thermal behavior, better reproducibility, simpler manufacturing process and higher reliability [9]. The AC resistance of the windings was reduced by controlling skin and proximity effects [10], with interleaving the primary and secondary layers in planar designs [11]. The magnetic field density (B) is needed to be kept below a reasonable value to avoid excessive core loss in the ferrite core. This is a serious limitation imposed from current materials to the design of magnetics for high-frequency power electronics. With equation (1) suggested in [12], we calculated the maximum magnetic field density (B_p) of 43.1mT at rated operating condition, which is still far below the saturation magnetic field density of N95 core material chosen for this design.

$$B_{\mathrm{p}} = \frac{V_{\mathrm{p}}}{4fNA_{\mathrm{min}}} \tag{1}$$

In this equation, V_{p} is the peak value of the square wave voltage, f is the fundamental frequency of the square wave, N is the number of the turns and A_{min} is the minimum core cross section.

Finite element analysis tool (COMSOL) was used to investigate the behavior of the transformer operating at 300 kHz. Fig. 3(a) shows the non uniform distribution of the magnetic field density inside the core. The average value of B from simulation was

Tab. 1: Specifications of the micro-converter

Parameter	Value
Rated Input Voltage	33 V
Max. Input Voltage	40 V
Max. Input Current	10 A
DC BUS Voltage	350 $\pm$ 10%
Switching Frequency	300 kHz

ISBN 978-3-8007-4646-0

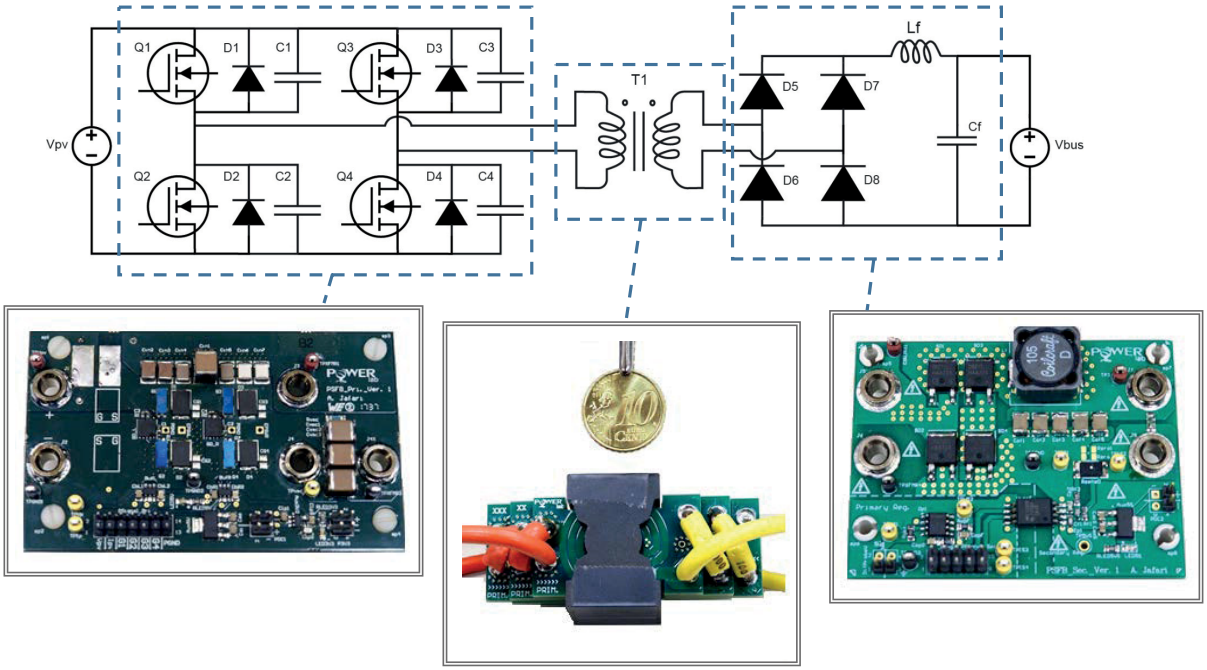

Fig. 2: Phase-shifted full-bridge topology and the designed micro-converter

limited to 14 mT under full-load conditions, which avoids excessive core loss, resulting in a smaller temperature rise. The current density analysis of the transformer windings shown in Fig. 3(b) was used to investigate skin and proximity effects in the windings, as well as the effect of interleaving on the AC resistance in this design. Based on the simulation, the AC resistance of 7.4 mΩ was calculated for the internal windings, and the measured value for the prototype was 27.5 mΩ at 300 kHz. The difference is due to the added resistance of connection wires between the stacks and also to the primary and secondary circuits. The PSFB topology allows a bi-directional core excitation [5], which combined with the high-frequency operation, led to a compact transformer design reaching a power density larger than 6 kW/l.

Fig. 4 shows the implemented planar transformer with its specification detailed in Tab. 2. To reach a 12-fold voltage step-up, a turns-ratio of 5:60 was selected and implemented with 5 stacks of 1:12 turns in series. To reduce the AC resistance, especially on the primary side which carries the high current, we doubled the primary turns (in parallel) and increased the copper thickness to 140 μm (4 oz).

Tab. 2: Specifications of the planar transformer

Parameter	Value
Turns ratio (N_p:N_s)	5:60
Core	PQ 32/20 and PQ 32/30 N95
AC resistance (from primary side)	27.5 mΩ
Leakage inductance (L_r)	215 nH

4. Experimental results

The primary-side inverter consisted of 4 EPC2022 devices paralleled with 4 low-voltage-drop schottky diodes FSV20150V. The rectifier at secondary consisted of 4 IDM02G120C5 SiC schottky diodes.

As discussed in section 2, the topology allows for soft-switching of primary-side transistors. Fig. 5 to Fig. 8 show the transients of switching for the transistors Q2 and Q4 respectively at the rated condition of the converter. Measuring the current at the high-frequency current loop, deteriorated the circuit

ISBN 978-3-8007-4646-0

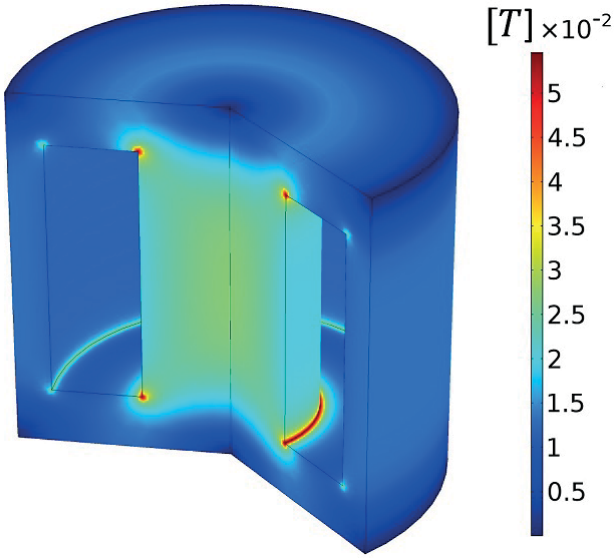

(a) Magnetic field density in the core; The average value is kept below 14mT to avoid excessive core loss at high frequency

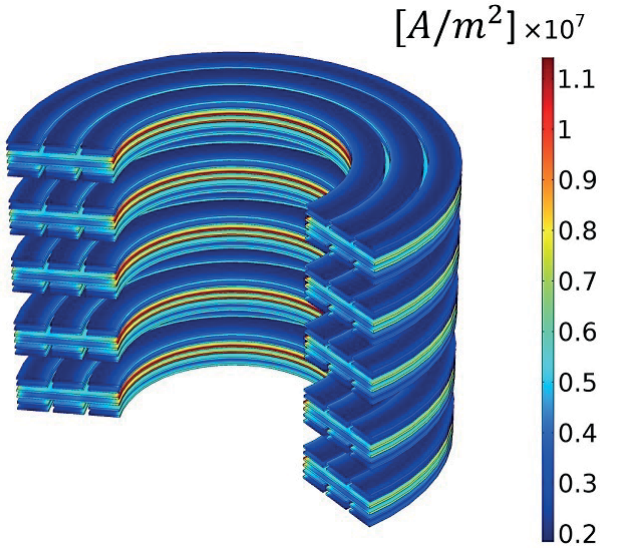

(b) Current density in the windings; Interleaving of primary and secondary layers reduces the AC resistance

Fig. 3: Finite element analysis of the designed transformer at rated condition at 300 kHz

performance, therefore we measured V_{ds} vs. V_{gs} to evaluate the switching behavior of the low-side transistors [13]. As explained in [8], PSFB topology does not offer similar conditions for achieving soft-switching in both legs. The condition to achieve soft-switching for the lagging leg (consisting of Q3 and Q4 transistors) is more restricted than the leading leg (Q1 and Q2), since only the leakage inductance of the transformer participates in soft-switching of the lagging leg, while for the leading leg, both the leakage inductance of the transformer and secondary-side filter inductor contribute to soft-switching. Fig. 5 shows the turn-on switching transient for Q2 as it achieves ZVS. In Fig. 6 the turn-off transient for Q2 occurs with zero current, achieving therefore ZCS. Fig. 7 and Fig. 8 show the turn-on and turn-off for Q4. Partial ZVS and full ZCS were achieved on turn-on and turn-off respectively.

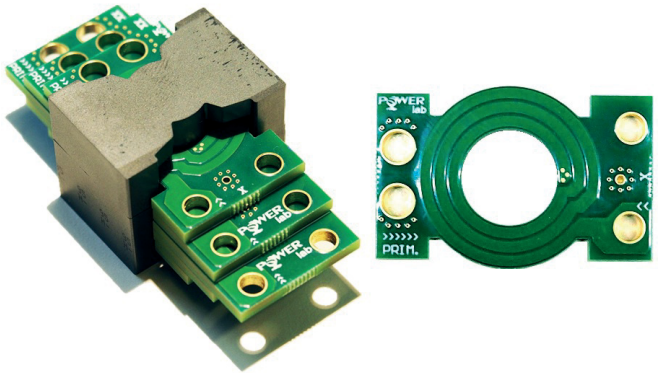

Fig. 4: Stacked PCB layers of high-frequency planar transformer prototype (left) and a single stack (right)

Temperature measurement of the transformer under rated operation, performed at room temperature, is shown in Fig.9. The highest temperature of the converter (87.7°C) occurs at the the connection points of the transformer to the primary-side inverter. The temperature of the primary and secondary circuits never exceeded 67°C. It is important to mention that this superior thermal performance was achieved without using any heatsinks or forced cooling.

Using an electronic load of 580 Ω, the efficiency and output power (P_o) of the converter at maximum phase shift for different input voltages (V_{pv}) are illustrated in Fig. 10. The converter maintains an efficiency of more than 93% for a wide range of output powers and input voltages without any efficiency drop at low voltage conditions (the loss on gate drivers and digital signal processor were considered negligible and thus not taken into account).

ISBN 978-3-8007-4646-0

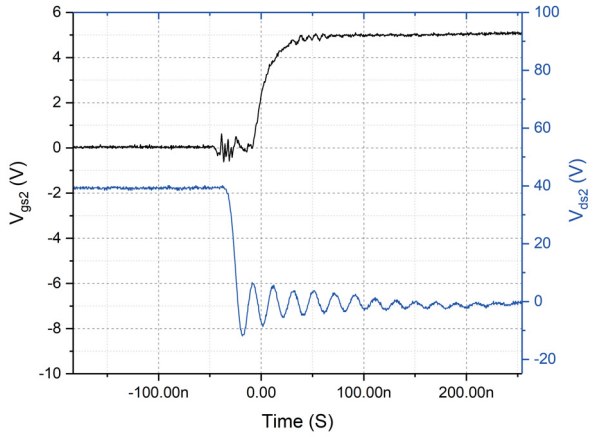

Fig. 5: Turn-ON switching transient of Q2 FET, achieving ZVS

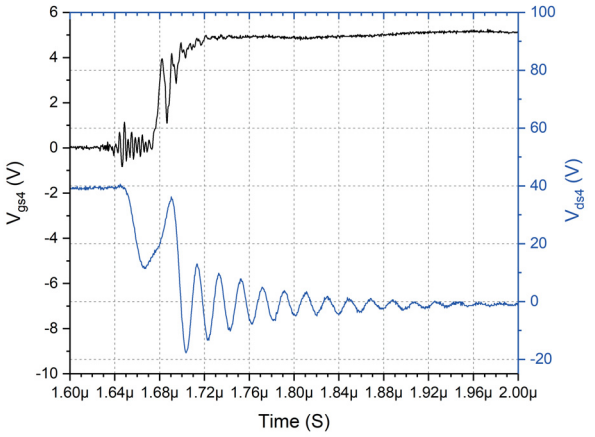

Fig. 7: Turn-ON switching transient of Q4 FET, achieving partial ZVS

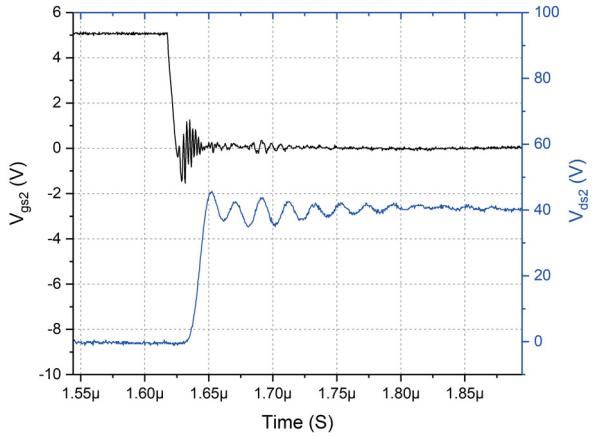

Fig. 6: Turn-OFF switching transient of Q2 FET, achieving ZCS

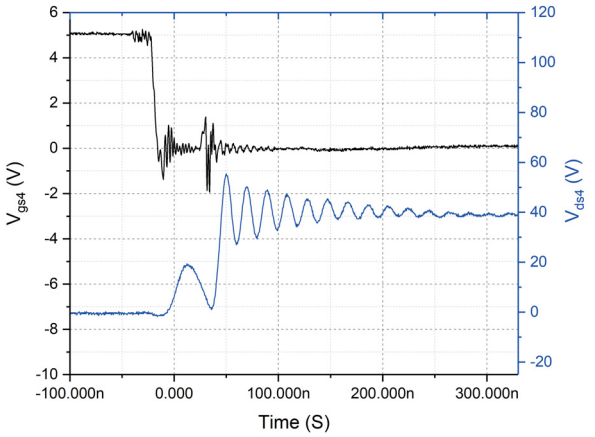

Fig. 8: Turn-OFF switching transient of Q2 FET, achieving ZCS

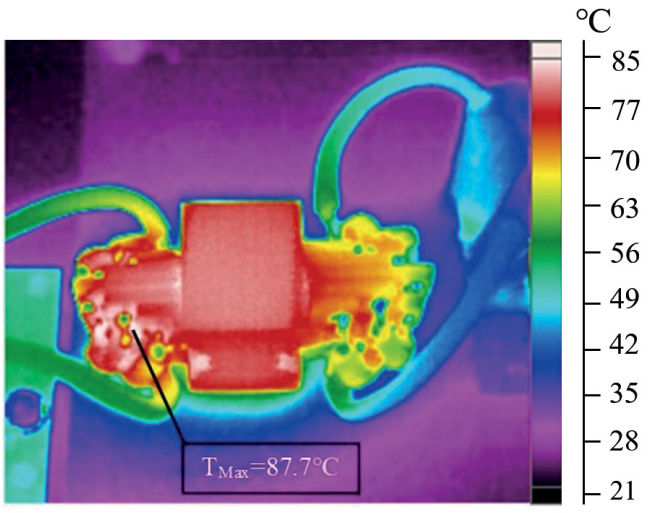

Fig. 9: Temperature of high-frequency transformer; the hottest point is the connection point of the transformer to the primary-side inverter

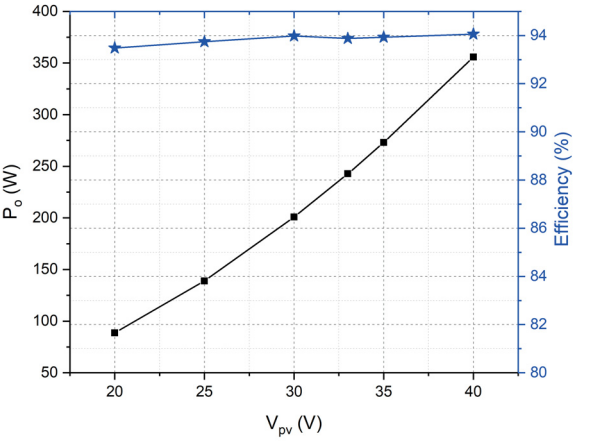

Fig. 10: Efficiency of the converter at maximum phase shift for various input voltages

ISBN 978-3-8007-4646-0

5. Conclusion

In this paper, a high-frequency high step-up single-stage DC-DC converter based on GaN HEMTs was presented for PV applications and emerging DC grids. A high-frequency planar transformer was designed to achieve high step-up in the voltage in a single-stage micro-converter. An overall converter efficiency of more than 93% for a wide range of input voltages and output powers was achieved.

Acknowledgement

The authors acknowledge the kind help and advice from Peter Brühlmeier and Roland Wetter on assembling the prototype of the converter.

6. References

[1] E. I. Batzelis, G. E. Kampitsis, S. A. Papathanassiou, and S. N. Manias. Direct MPP Calculation in Terms of the Single-Diode PV Model Parameters. *IEEE Transactions on Energy Conversion*, 30(1):226–236, March 2015.

[2] A. Ghaffari, M. Krsti, and S. Seshagiri. Power Optimization for Photovoltaic Microconverters Using Multivariable Newton-Based Extremum Seeking. *IEEE Transactions on Control Systems Technology*, 22(6):2141–2149, November 2014.

[3] A. Jain, S. Jain, and D. K. Palwalia. Stability enhancement of DC-DC converters using robust droop control scheme and circulating current elimination in DC micro-grid. In *2016 IEEE 7th Power India International Conference (PIICON)*, pages 1–6, November 2016.

[4] M. Wu, L. J. Sun, H. Zhang, W. Wang, and G. M. Luo. Research on optimal storage capacity of DC micro-grid system in PV station. *The Journal of Engineering*, 2017(13):859–864, 2017.

[5] M. Kasper, M. Ritz, D. Bortis, and J. W. Kolar. PV Panel-Integrated High Step-up High Efficiency Isolated GaN DC-DC Boost Converter. In *Intelec 2013; 35th International Telecommunications Energy Conference, SMART POWER AND EFFICIENCY*, pages 1–7, October 2013.

[6] Sam Abdel-Rahman. Resonant LLC converter: Operation and design. *Infineon Technologies North America (IFNA) Corp.*, 2012.

[7] Jiangheng Lu and A. Khaligh. 1kw, 400v/12v high step-down DC/DC converter: Comparison between phase-shifted full-bridge and LLC resonant converters. In *2017 IEEE Transportation Electrification Conference and Expo (ITEC)*, pages 275–280, June 2017.

[8] Xinbo. Ruan. *Soft-switching PWM full-bridge converters : topologies, control, and design*. 2014.

[9] M. A. Saket, N. Shafiei, and M. Ordonez. Planar transformer winding technique for reduced capacitance in LLC power converters. In *2016 IEEE Energy Conversion Congress and Exposition (ECCE)*, pages 1–6, September 2016.

[10] Irma VILLAR. *Multiphysical Characterization of Medium-Frequency Power Electronic Transformers*. PhD thesis, COLE POLYTECHNIQUE FDRALE DE LAUSANNE, EPFL, Switzerland, 2010.

[11] Z. Ouyang, O. C. Thomsen, and M. A. E. Andersen. Optimal design and tradeoffs analysis for planar transformer in high power DC-DC converters. In *The 2010 International Power Electronics Conference - ECCE ASIA -*, pages 3166–3173, June 2010.

[12] Edward Hebner. Soft Ferrites and Accessories Data Handbook (Ferroxcube), 2013.

[13] Alex Lidow, Johan Strydom, Michael de Rooij, and David Reusch. *GaN Transistors for Efficient Power Conversion*. WILEY, USA, second edition, 2015.